Electrochimica Acta, Vol. 33, No. 10, pp. 1431–1437, 1988.
Printed in Great Britain.

0013–4686/88 $3.00 + 0.00

THE ROLE OF A SLOW PHASE FORMATION PROCESS IN THE GROWTH OF ANODIC SILVER OXIDE LAYERS IN ALKALINE SOLUTIONS—I. ELECTROFORMATION OF Ag(I) OXIDE LAYER

J. GOMEZ BECERRA, R. C. SALVAREZZA and A. J. ARVIA

Instituto de Investigaciones Fisicoquímicas Teóricas y Aplicadas (INIFTA), Facultad de Ciencias Exactas, Universidad Nacional de La Plata, Sucursal 4, Casilla de Correo 16, (1900) La Plata, Argentina

(*Received* 6 *January* 1988)

Abstract—The anodic electroformation of silver (I) oxide layer on polycrystalline silver electrodes in 0.1 M NaOH was studied by using potentiodynamic and potentiostatic techniques. The growth of the silver oxide layer under a linear potential sweep or potential step measurements involves as a first step the electroformation of Ag_2O or AgOH monolayer at potentials close to the Ag/Ag_2O reversible electrode potential. This monolayer grows through a solid diffusion mechanism to form a 3-D primary silver (I) oxide. Subsequently the building up of a secondary silver (I) oxide layer is clearly noticed when the potential exceeds 0.24 V (*vs sce*). The formation of this layer can be described in terms of an instantaneous nucleation and 3-D growth mechanism under diffusion control. The ageing effects at the primary layer level decreases the nucleation rate so that for the growth of the secondary layer an intermediate situation between instantaneous and progressive nucleation under diffusion control can be observed. The secondary silver (I) oxide layer can be related to the aged silver (I) oxide species previously reported.

INTRODUCTION

The electrochemical behaviour of Ag electrodes in alkaline solutions has been extensively studied through voltammetry[1–6], chronoamperometry[7, 8] and chronopotentiometry[9, 10], and the oxide phases formed on the electrode surface were analysed by using X-ray diffraction[10], scanning electron microscopy[10], Raman spectroscopy[11] and ellipsometric measurements[5, 9]. There is agreement that the first electrooxidation level of Ag in alkaline solutions yields a thick Ag_2O layer on the electrode surface[1–11]. The voltammetric response of this process implies at least three well defined peaks, a fact which suggest that the formation of Ag_2O is a multistage process[1, 2]. Although the first stage has been associated with the electroformation of a monolayer of either Ag_2O or AgOH[12], there is still no agreement about the reaction related to the second stage which has been assigned to the electroformation of either base Ag_2O layer[3] or O-layer trapped into the Ag surface[13] (O–Ag alloy), or to Ag electrodissolution as $Ag(OH)_2^-$[2, 14]. X-ray diffractogram and SEM micrographs indicate that the growth of a base Ag_2O layer is followed by the buildup of a secondary layer[10]. Finally, the third stage of Ag_2O electroformation which corresponds to the most anodic current peak, has been unambiguously assigned to the 3-D growth of the Ag_2O phase although results from few chronoamperometry studies pointed out that no nucleation and growth control can be associated with that reaction[7, 8]. According to these results the growth of the Ag_2O phase is kinetically limited by diffusion/migration of silver ions through the randomly oriented silver oxide basal layer[7]. Evidence for nucleation and growth as the rate controlling step for Ag_2O formation through silver anodization in base solution was also presented[14], although no attempts were made at the time being to fit the current transients in terms of conventional nucleation and growth models[14]. The presence of inflections in the current transients and supposedly artifacts in the voltammetric measurements were attributed as proper characteristics of reformed silver electrode surfaces consisting of a large number of overlapped nuclei with complex diffusional paths[8]. In relation to the third stage of Ag_2O growth ageing processes occurring in the potential range of Ag_2O formation were also reported[1].

This paper is devoted to investigate the electroformation of the Ag(I) oxides from voltammetric and potentiostatic measurements under controlled experimental conditions. Unambiguous evidence for nucleation and growth processes at certain stages of the Ag(I) oxide layer electroformation is obtained. The new Ag_2O phase resulting from the nucleation and 3-D growth process is responsible of the ageing effects at the anodically formed silver oxide layer, previously reported[1].

EXPERIMENTAL

Working electrodes were made of polycrystalline (pc) Ag (99.99%) rods axially embedded in Araldite holders to obtain circular exposed areas of 0.05 cm^2 apparent area. The electrodes were mechanically polished starting with fine grained emery paper followed with alumina paste of 1 μm diameter to produce mirror surfaces. Before the electrochemical measurements the electrodes were degreased with alcohol and rinsed with triply distilled water. Special care was taken to avoid crevices between Ag rods and Araldite holders which

could lead to artifacts in the voltammetric and potentiostatic measurements. The counter electrode was a large Pt sheet located in a separate cell compartment. The potential of the working electrode was measured against a saturated calomel electrode (*sce*) connected to the working electrode cell compartment through a Luggin–Haber capillary tip. Potentials in the text are referred to the *sce*. The electrolyte solutions were xM NaOH ($10^{-1} \leqslant x \leqslant 1$) prepared by using triply distilled water and AR chemicals. Solutions were bubbled with purified nitrogen for 3 h prior to the electrochemical measurements. The latter consisted only of a single triangular potential scan between the cathodic ($E_{s,c}$) and the anodic ($E_{s,a}$) switching potentials. Repetitive potential scans were specifically avoided as the electroreduction of the silver oxide layer results in reformed[8] Ag surfaces made of a large number of overlapping nuclei with complex diffusional paths. Thus, a new fresh polished Ag electrode was used for each measurement. Current transients under a constant potential step were recorded in the conventional way by using the perturbing potential programs described in the text. In all these cases the Ag electrodes were held at $E_{s,c} = -1.30$ V, for 60 s, to start each electrochemical run with a reproducible electroreduced silver surface. All measurements were made at $T = 25°C$.

RESULTS

Voltammetric data

The apparent current density–potential (j–E) profiles recorded for a pc Ag electrode in 0.1 M NaOH at $v = 0.5 \times 10^{-3}$ V s^{-1} between $E_{s,c} = -1.30$ V and $E_{s,a} = 0.60$ V show in the positive potential going scan a small peak (A'_1) at 0.21 V preceding peak A''_1 at 0.28 V (Fig. 1). The latter is followed by a decreasing current which extends to 0.52 V. At potentials greater than 0.52 V a narrow and large peak (A_2) at 0.55 V is observed. In the negative potential going scan a broad cathodic peak (C_2) at 0.47 V shows up followed by an anodic current which becomes cathodic at potentials lower than 0.20 V. Finally, a large and narrow peak (C_1) appears at 0.10 V. Runs performed at higher v (*eg* $v = 0.1$ V s^{-1}) between $E_{s,c} = -1.30$ and $E_{s,a} = 0.45$ V, exhibit an additional small peak (A_{1m}) located at 0.165 V (Fig. 2), the charge density for the latter (q_{1m}) being close to 400 μC cm^{-2}.

Voltammograms were also run at $v = 5 \times 10^{-3}$ V s^{-1} from $E_{s,c} = -1.30$ V and $E_{s,a}$ changed stepwise in the positive direction (Fig. 3) in order to inspect complementary anodic and cathodic reactions. Thus, when $E_{s,a} = 0.20$ V only an anodic current plateau (A_{1m}) and a complementary broad cathodic peak (C_{1m}) can be seen (Fig. 3a). Likewise, for $E_{s,a} = 0.22$ V (Fig. 3b) plateau A_{1m} extends up to the base of peak A_1, and simultaneously the electroreduction charge increases in the potential region of peak C_{1m}. In addition, when $E_{s,a} = 0.25$ V (Fig. 3c), peak A'_1 is observed and peak C'_1 is shifted negatively as $E_{s,a}$ is progressively set more positive. These facts are accompanied by a new cathodic current hump (C''_1) at the negative potential side. Finally, when $E_{s,a} = 0.25$ V peak A'_1 becomes completely developed (Fig. 3d). At this stage a vigorous stirring of the electrolyte solution produced no marked changes over the entire voltammetric profile. The subsequent increase in $E_{s,a}$ to 0.27 V, that is at the starting portion of peak A'_1, a hysteresis loop at the initiation of the negative potential going excursion can be clearly noticed (Fig. 3e). The complementary electroreduction voltammogram consists of a sharp peak C''_1 with a hump at its positive potential side. This hump is the remaining contribution of peak C'_1.

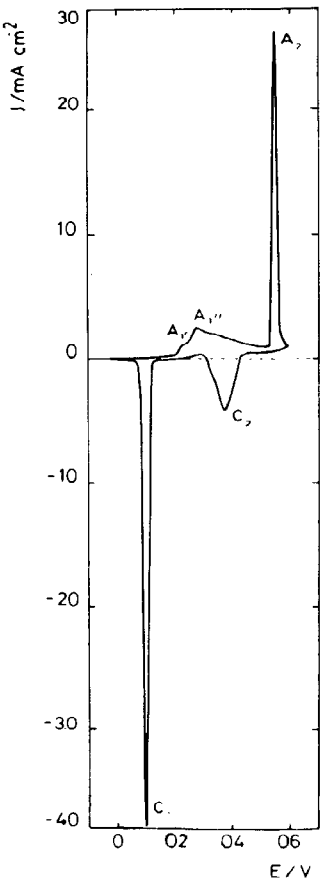

Fig. 1. j–E profile for a polycrystalline Ag electrode recorded between $E_{s,c} = -0.2$ V and $E_{s,a} = 0.6$ V at $v = 0.5 \times 10^{-3}$ V s^{-1} in 0.1 M NaOH.

Peak A_{1m} can be attributed to the electroformation of a monolayer of either AgOH or Ag_2O[12] which can be electroreduced within the potential range of peak C_{1m}, whereas, peaks A'_1, A''_1 and C'_1, C''_1 can be assigned to processes involved in the electroformation and electroreduction of bulk Ag_2O, respectively. Finally, peak A_2 is related to the formation of a Ag(II) oxide layer which is electroreduced to Ag_2O in the potential range of peak C_2.

Similar experiments made by changing v from 0.5×10^{-3} V s^{-1} to 0.1 V s^{-1}, results in the linear increase of the height of peak A''_1 with the square root of v (Fig. 4).

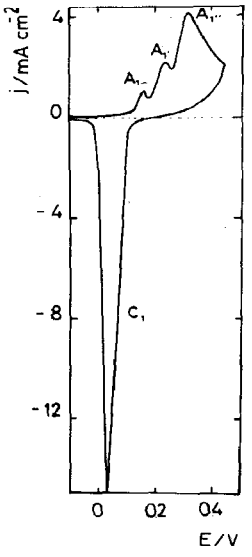

Fig. 2. j–E profile for a polycrystalline Ag electrode recorded between $E_{s,c} = -0.2$ V and $E_{s,a} = 0.45$ V at $v = 0.1$ V s^{-1} in 0.1 M NaOH.

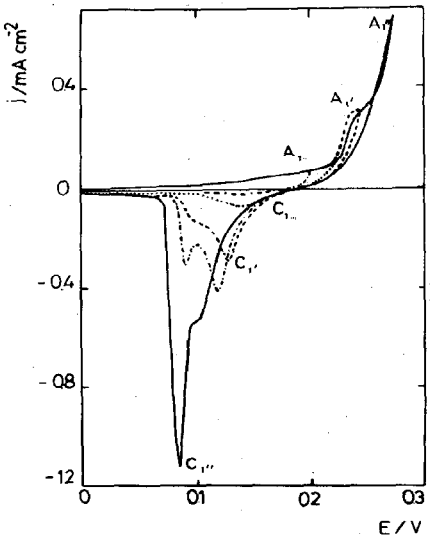

Fig. 3. j–E profiles for a polycrystalline Ag electrode recorded between $E_{s,c} = 0.0$ V and $E_{s,a}$ stepwise changed in the positive direction at $v = 5 \times 10^{-3}$ V s^{-1} in 0.1 M NaOH.

Potentiostatic current transients and stripping voltammetry data

Potentiostatic current transients were recorded by setting the applied potential at different values within the range of peaks A_{1m}, A'_1 and A''_1. For these runs the electrode pretreatment consisted of the following steps. Firstly, the electrode was held at -1.30 V for 60 s to start with the same reproducible electroreduced Ag surface. Later, the potential was stepped to $E_a = -0.30$ V (double layer region) for $t_a = 10$ s, and finally, it was held at a value of E_s comprised between 0.0 V and 0.35 V for current transient recording.

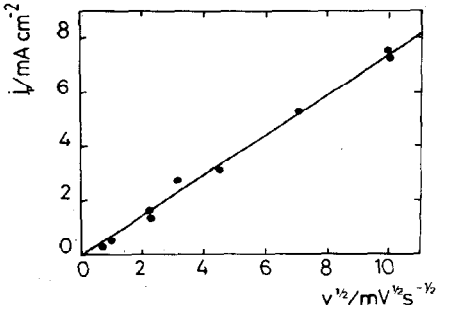

Fig. 4. Current density of peak A''_1 (j_p) *vs* $v^{1/2}$ plot. Electrolyte: 0.1 M NaOH.

When E_s is set in the potential range of peak A_{1m}, continuously decreasing current transients involving a small charge density ($q = 400\ \mu$C cm^{-2}) are obtained (Fig. 5a). Correspondingly, stripping cathodic voltammetry run from E_s to $E_{s,c} = -1.30$ V for the anodic layer formed after completion of the transient, shows up only peak C_{1m} (Fig. 5b). Analogous results comes out from those current transients recorded in the potential range of peak A'_1, although in this case larger q'_1 values are obtained (Fig. 6a). These data can be reasonably fitted to linear j *vs* $t^{-1/2}$ plots, except for $t < 0.4$ s (Fig. 7). This deviation can be attributed to the contribution of two processes undergoing at different rates. In agreement with this conclusion, for $t_s < 0.4$ s the corresponding stripping voltammograms show only peak C_{1m}, whereas for $t > 0.4$ s the development of peak C_1 masks the appearance of peak C_{1m} (Fig. 6b). Finally, when E_s lies in the potential range of peak A''_1, the current transient also falls continuously although a small hump for $t \to 0$ shows up (Fig. 8). The latter overlaps the initial falling current and becomes less remarkable as E_s is set gradually more positive. This hump is no longer observed for $E_s > 0.32$ V.

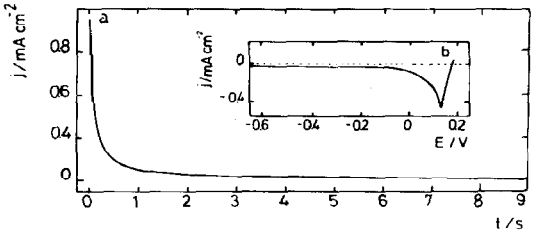

Fig. 5. (a) Current transient at constant potential ($E_s = 0.18$ V) for a polycrystalline Ag electrode recorded in 0.1 M NaOH after applying to the electrode the following pretreatment: $E_c = -1.30$ V, $t_c = 60$ s; immediately the electrode potential was held at $E_a = -0.30$ V for $t_a = 10$ s and finally, the potential was stepped to E_s for current transient recording. (b) Cathodic j–E profile recorded at $v = 0.05$ V s^{-1} after the completion of the transient shown in (a).

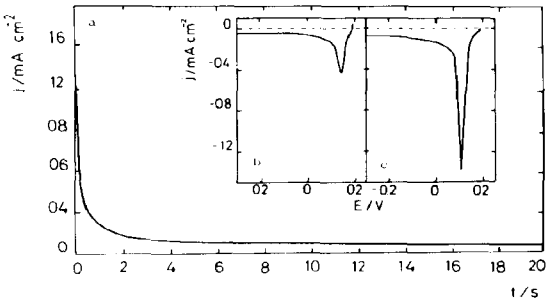

Fig. 6. (a) Current transient at constant potential for a polycrystalline Ag electrode (E_s = 0.19 V) recorded in 0.1 M NaOH after applying to the electrode the same pretreatment described in Fig. 5a. (b) Cathodic j E profile recorded at v = 0.05 V s^{-1} after t_s = 10 s. (c) Cathodic j–E profile recorded at v = 0.05 V s^{-1} after t_s = 600 s.

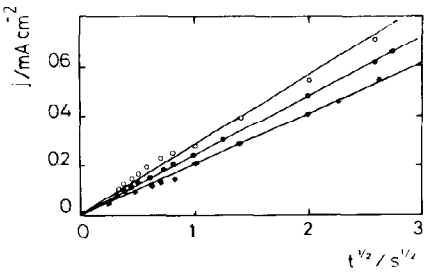

Fig. 7. j vs $t^{-1/2}$ plot for current transients recorded in the potential region of peak A'_1. (*) E_s = 0.20 V; (●) E_s = 0.21 V; (o) E_s = 0.22 V.

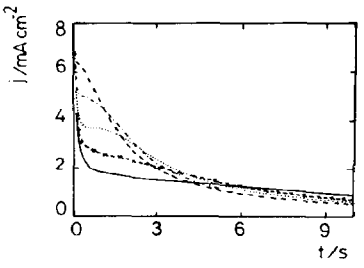

Fig. 8. Current transients at constant potential (E_s) recorded for a polycrystalline Ag electrode in 0.1 M NaOH after applying to the electrode the same pretreatment described in Fig. 5a. (——) E_s = 0.27 V; (×) E_s = 0.28 V; (···) E_s = 0.29 V, (–·–) E_s = 0.30 V; (– – –) E_s = 0.31 V.

The voltammetric electroreduction of the anodic layer formed for E_s = 0.30 V at short t_s, shows up a larger contribution of peak C'_1, and as t_s increases peak C''_1 develops at the negative potential side of peak C'_1 (Fig. 9). Therefore, it seems reasonable to relate the initial falling current and the hump resulting in the potentiostatic transient to peaks C'_1 and C''_1, respectively, appearing in the voltammogram.

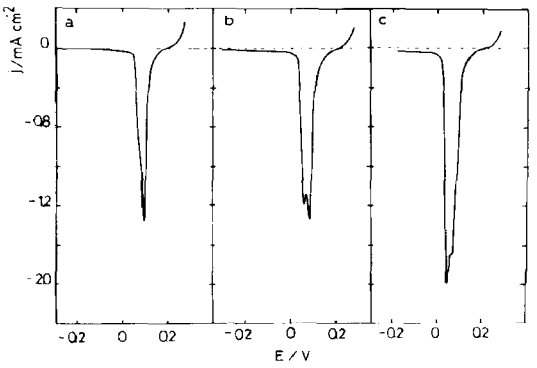

Fig. 9. Cathodic j–E profiles recorded at v = 0.05 V s^{-1} after anodization at E_s = 0.27 V for (a) t_s = 2 s; (b) t_s = 5 s; (c) t_s = 10 s.

In order to establish the relation between the portion of the current transient associated with the voltammetric peak A'_1, the Ag electrode was potential stepped from −1.30 V to E_a = 0.20 V for t_a = 120 s, to attain as much as possible the completion of those processes occurring in the potential range of peak A'_1, and later to hold the potential at an E_s value set between 0.27 V and 0.315 V for current transient recording. In this case, the initial decreasing current diminishes considerably and peaked current transients are obtained (Fig. 10a). These current transients exhibit a maximum, I_M, at the time, t_M, and later decrease slowly approaching a limiting current. In these experiments as E_s is set more positive, I_M increases, and t_M decreases, but independently of it, all transients approach the same current for $t \to \infty$. Finally, for E_s set at 0.20 V and t_a = 600 s, the fast initial current decrease can be practically suppressed (Fig. 10b). In this case for t_a = 600 s, I_M results smaller than that already found for t_a = 120 s. It is interesting to notice that for t_a = 120 s and t_a = 600 s the middle rising section of the current transients fulfills linear j vs $t^{1/2}$ relationship with a slope depending on E_s (Fig. 11). Furthermore, for t_a = 600 s (Fig. 11a) the linear j vs $t^{1/2}$ plot intercepts the origin of coordinates, whereas for t_a = 120 s (Fig. 11b) a finite current for t = 0 is found. On the other hand, the tails of current transients, from $t > t_M$ to $t \to \infty$, satisfy j vs $t^{-1/2}$ linear plots (Fig. 12a and b), with the same slope for different electrolyte concentrations in the 10^{-1} M < c_{NaOH} < 1 M range.

DISCUSSION

The facts that the potential of peak A_{1m} is close to the reversible potential of the Ag/Ag_2O redox couple in 0.1 M NaOH, E_r = 0.163 V (*vs sce*), and that the corresponding charge density, q_{1m} is 400 μC cm^2, indicate that the first electrooxidation stage involves a compact monolayer of O-containing surface species[15]. This reaction can be written as follows:

$$Ag + H_2O = AgOH + H^+ + e^-, \quad (1a)$$

$$Ag + OH^- = AgOH + e^-, \quad (1b)$$

$$2AgOH = Ag_2O(H_2O). \quad (2)$$

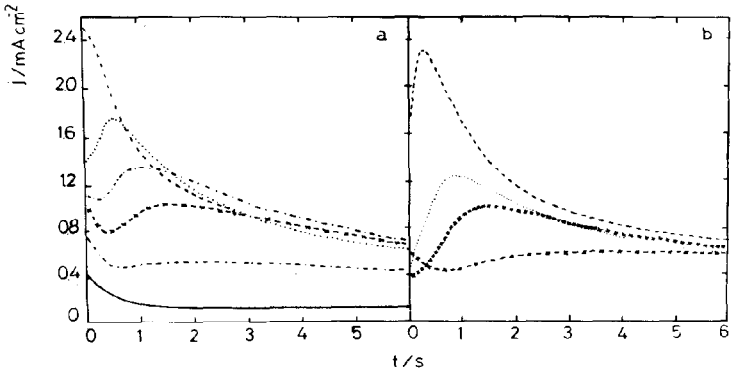

Fig. 10. (a) Current transients at constant potential (E_s) recorded for a polycrystalline Ag electrode in NaOH 0.1 M after applying to the electrode the following pretreatment: $E_c = -1.3$ V; $t_c = 60$ s; later stepped to $E_a = 0.19$ V for $t_a = 120$ s and finally stepped to E_s for current transient recording. (——) $E_s = 0.26$ V; (– – –) $E_s = 0.278$ V; (– × –) $E_s = 0.28$ V; (– · –) $E_s = 0.285$ V, (···) $E_s = 0.30$ V, (– – –) $E_s = 0.315$ V. (b) *idem* as (a) for $t_a = 600$ s. (– × –) $E_s = 0.28$ V; (× × ×) $E_s = 0.29$ V; (···) $E_s = 0.30$ V; (– – –) $E_s = 0.315$ V.

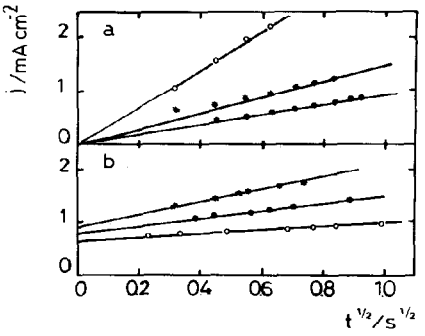

Fig. 11. (a) j *vs* $t^{1/2}$ plots for the middle rising portions of the current transients showed in Fig. 10b. (●) $E_s = 0.29$ V; (*) $E_s = 0.30$ V; (o) $E_s = 0.315$ V. (b) j *vs* $t^{1/2}$ plots for the middle rising portions of the current transients showed in Fig. 10a. (o) $E_s = 0.28$ V; (●) $E_s = 0.285$ V; (*) $E_s = 0.30$ V.

Accordingly, a monolayer of AgOH can be formed either through electrodecomposition of H_2O (Step 1a) or through OH^--ion discharge (Step 1b). This monolayer can also be conceived as a hydrous Ag_2O layer.

In contrast to the first electrooxidation stage, reactions occurring in the potential range of peak A'_1 are still found to be ambiguous. Based upon different arguments the reaction has been assigned either to the electroformation of a Ag_2O base layer[3], or to Ag electrodissolution as $Ag(OH)_2^-$[2–14], or to the formation of a sublayer of O-atom trapped into the Ag surface[13]. The present results provide a new perspective to consider which of those three possible processes is involved in the electrochemical reaction associated with peak A'_1. For this purpose let us try to find out the most likely reaction model to explain the current transients data resulting under different conditions.

The continuously decreasing part of the potentiostatic current transients recorded in the potential range of peak A'_1 fit linear j *vs* $t^{-1/2}$ plots (Fig. 7). This type of kinetic law suggests at a first sight a diffusional controlled process, as given by the equation:

$$j(t) = \frac{zFD^{1/2}}{\pi^{1/2}t^{1/2}}c_s \tag{3}$$

where D is the diffusion coefficient of the reacting species its concentration being c_s. The formal validity of Equation (3) might indicate that the Ag electrodissolution involves a rate determining transport of cations to solution. This possibility, however, can be immediately discarded as the rates of the reactions related to both peaks A'_1 and C'_1 undergoing either voltammetrically or potentiostatically, become practically independent of the solution stirring. Furthermore the values of the diffusion coefficient derived from the slope of the straight lines, of the j *vs* $t^{-1/2}$ plots for the solubility of Ag_2O taken as $c_s = 1.5 \times 10^{-7}$ mol cm^{-3}, is $D = 7.0 \times 10^{-2}$ cm^2 s^{-1}, a figure which is completely unrealistic for ionic diffusion in aqueous solution. On the other hand, the fact that the product of the early stages of the anodic layer formation, that is the product formed in the potential range of peak A'_1, can be electroreduced just in the potential range of peak C_{1m}, indicates the close identity between this anodic product and that related to the first Ag_2O monolayer. Therefore, these facts provide a strong support of the assignment of a common product to the reaction related to peak A'_1 and to the formation of a base Ag_2O. Hence, the formation of an O–Ag alloy at the early stages of the anodic process is unlikely. Otherwise, the kinetics of the Ag_2O layer thickening appears to be controlled by the diffusion of Ag^+ ions through the thin and probably highly defective Ag_2O monolayer. This interpretation is consistent with the fact that practically all the charge involved in peak A'_1 remains stored at the electrode ($q'_{A_1}/q'_{C_1} = 1.1$) and only a small portion of it appears as soluble Ag^+ ionic species[5]. In this case, the average thickness of the anodic layer where Ag^+ ion diffusion takes place can be estimated from the charge density, q'_{A_1}, resulting from the integration of current transients according to:

$$h = \frac{Mq'_{A_1}}{zF\rho}, \tag{4}$$

where M and ρ are the molecular weight ($M = 231.7\ g\ mol^{-1}$) and the density ($7.143\ g\ cm^{-3}$) of the Ag_2O, respectively. The value of h derived from the current transients shown in Fig. 6a is 8.3 nm, a figure which should be presumably slightly higher for a hydrous anodic layer structure if the M/ρ ratio for the latter is slightly greater than that for pure Ag_2O.

Let us now consider the interesting data concerning peaks A_1'' and C_1''. There is agreement among different authors in the sense that these peaks correspond to the electroformation (A_1'') and the electroreduction (C_1'') of a certain type of Ag_2O, *eg* that which most likely corresponds to the secondary layer detected by X-ray diffraction and electron microscopy[10] and which quite likely becomes responsible for the ageing effect earlier detected through voltammetry[1]. Various facts such as the peaked current transients with falling current approaching a common current value for $t \to \infty$ which is independent of E_s (Figs 10a and b), the voltammetric loop observed at the earlier stages of the peak A_1'', the j *vs* $v^{1/2}$ linear plot obtained for peak A_1'' (Fig. 4), and the absence of a marked influence of the solution stirring on the current transients and voltammetric profiles, are consistent with a kinetic interpretation for the electroformation of a secondary Ag_2O layer based on a nucleation and 3-D growth mechanism under diffusion control at the oxide layer. This conclusion is also sustained by the appearance of isolated 3-D growth centres for the secondary Ag_2O layer growth as detected by SEM[10]. Accordingly, the proposed mechanism, under the assumptions of an instantaneous nucleation, leads to the apparent current density as given by the expression:

$$j(t) = \frac{zFD_s^{1/2}c_{Ag^+}}{\pi^{1/2}t^{1/2}}[1.0 - \exp(-\pi K_e D_s N_0 t)]$$

$$= \frac{P_1}{t^{1/2}}[1.0 - \exp(-P_2 t)], \qquad (5)$$

and for a progressive nucleation:

$$j(t) = \frac{zFD_s^{1/2}c_{Ag^+}}{\pi^{1/2}t^{1/2}}[1.0 - \exp(-\pi K_e' D_s N_0 \alpha t^2)]$$

$$= \frac{P_1}{t}[1.0 - \exp(-P_3 t^2)], \qquad (6)$$

where $zFD_s^{1/2}c_{Ag^+}/\pi^{1/2} = P_1$; $\pi K_e D_s N_0 = P_2$ and $\pi K_e' D_s N_0 \alpha = P_3$; D_s is the diffusion coefficient of Ag^+ ions in the oxide layer; N_0 is the number of sites available for nucleation; αN_0 is the nucleation rate and K_e and K_e' are proportionality constants.

For $t \to 0$ Equations (5) and (6) result:

$$j(t) = P_1 P_2 t^{1/2}, \qquad (9)$$

$$j(t) = P_1 P_3 t^{3/2}, \qquad (10)$$

whereas, for $t \to \infty$,

$$j(t) = P_1/t^{1/2}. \qquad (11)$$

The limiting Equations (9) and (11) are reasonably fulfilled by the experimental results (Figs 11 and 12). It is clear that the instantaneous nucleation approach is only valid for $t_a = 120$ s, as seen through the dimensionless plots shown in Fig. 13a. In contrast the results for $t_a = 600$ s (Fig. 13b) apparently reflect an intermediate situation between instantaneous and progressive nucleation, as it has already been observed for other systems[18]. This transition from instantaneous to progressive nucleation in the anodic layer growth as t_a increases beyond a certain value can be explained through the increasing contribution of the ageing effects at the primary layer level. Certainly this contribution should be more remarkable as t_a increases. Hence, as the contribution of ageing effects increases the nucleation rate associated with the growth of the secondary layer diminishes.

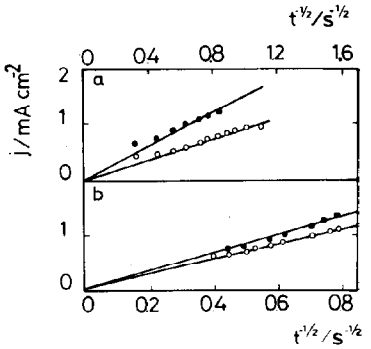

Fig. 12. (a) j *vs* $t^{-1/2}$ plots for the decaying portions of the current transients showed in Fig. 10b. (o) $E_s = 0.28$ V; (●) $E_s = 0.315$ V. (b) j *vs* $t^{-1/2}$ plots for the decaying portions of the transients showed in Fig. 10a. (o) $E_s = 0.30$ V; (●) $E_s = 0.315$ V.

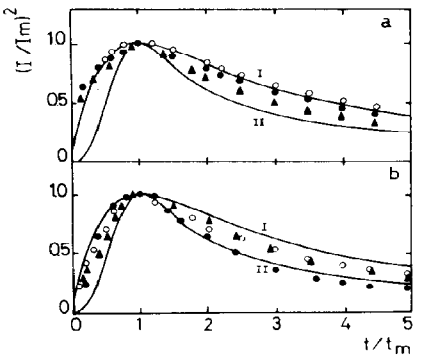

Fig. 13. Dimensionless $[(I/I_M)^2$ *vs* $(t/t_M)]$ plots for (I) instantaneous nucleation, (II) progressive nucleation: (a) $t_a = 120$ s; (o) $E_s = 0.28$ V; (●) $E_s = 0.285$ V; (▲) $E_s = 0.30$ V. (b) $t_a = 600$ s; (o) $E_s = 0.29$ V; (▲) $E_s = 0.30$ V; (●) $E_s = 0.315$ V.

Another important fact for discussion concerns the independance of the value of P_1 on the OH^- ion concentration. This fact confirms that Ag^+ ions are the predominantly mobile entities in the growing oxide layer as it has been earlier suggested[19]. In this case, the concentration (c_{Ag^+}) of silver ions at the metal–oxide interface can be estimated by using $D_s = 4 \times 10^{-12}\ cm^2\ s^{-1}$[20] and P_1 values derived from the slope of the straightlines of the j *vs* $t^{-1/2}$ plots (Fig. 10). Values of c_{Ag^+} equal to $2.9 \times 10^{-3}\ mol\ cm^{-3}$ and $4.3 \times 10^{-3}\ mol\ cm^{-3}$, for $E_s = 0.29$ V and $E_s = 0.315$ V, respectively are obtained. It can be noticed that these

c_{Ag^+} values are greater than those which have been obtained through *ac* impedance measurements as it should be expected because the former data correspond to non stationary conditions, whereas the latter refer to steady state conditions for the oxide layer growth[19].

Additional data can be derived from the slope of the j *vs* $t^{1/2}$ linear plots (Fig. 11b) on the basis of Equations (9) and (11). Thus the N_0 value can be estimated by taking $D_s = 4 \times 10^{-12}\ cm^2\ s^{-1}$ and $K_e = (8\pi M c_{Ag^+}/\rho)^{1/2}$. The values of N_0 are about $1 \times 10^{11}\ cm^{-2}$. Thus, in the 0.29–0.315 V range these nucleation centers can be directly related to sites exclusively located on the primary anodic oxide layer. The possibility that the nucleation centers be located at the silver surface appears to be quite unlikely because the growth of the secondary layer becomes independent of the electrode surface treatment, *eg* electropolished, or mechanically polished[10].

The physical picture underlying the proposed model considers that in the potential range of peak A_1'' a supersaturation concentration of Ag^+ ions is reached at the outer plane (o) of the Ag_2O primary layer, which leads to 3-D nuclei formed instantaneously. Therefore, the earlier stages of this reaction can be represented as follows:

$$Ag^+(solid) \rightarrow Ag^+(o), \quad (12)$$

$$Ag^+(o) + OH^- + N \rightarrow AgOH\ (N), \quad (13a)$$

$$Ag^+(o) + H_2O + N \rightarrow AgOH\ (N), \quad (13b)$$

$$n\,AgOH + N \rightarrow (AgOH)_n\ (N), \quad (14)$$

where N denotes a preferred site in the primary layer and n the number of piled up species forming the growing layer. This sequence of reactions implies a Ag^+ ion transfer from the metal lattice to the metal–solution interface, AgOH incipient nuclei formation either through OH^- ions or H_2O molecules and finally, the AgOH layer growth as denoted by Equation (14). As the nuclei expands hemispherical diffusion zones build up around the nuclei, and when the diffusion zones overlap the rate of Reaction (12) becomes determined by the rate transport of Ag^+(o) ions to growing centers through diffusion perpendicularly to the electrode surface. Hence, as $t \rightarrow \infty$ the ion transport in the anodic layer becomes a semi-infinite linear diffusion controlled process.

From the present work further conclusions can be drawn in relation to previously reported data. Thus, it is clear that the continuously decreasing current transients for the anodic layer formation may arise from the sum of different processes which mask the peaked transients characteristics of nucleation and growth. Therefore, in this case a special care must be taken in order to exclude the nucleation and growth as rate controlling reaction. Otherwise, the cathodic peak C_1'' which develops at the negative side of peak C_1' definitely corresponds to the electroreduction of an "aged" Ag(I) oxide layer[1] which was produced through the nucleation and growth controlled mechanism. Finally, earlier ellipsometric data showing that the degree of porosity of the Ag_2O layer depended on the potential sweep rate[5] can now be explained. This effect arises from the fact that different degrees of overlapping of growing nuclei in the secondary layer can be achieved according to the potential sweep rate employed in the potentiodynamic measurements.

In conclusion, for the first time unambiguous evidence is presented for the participation of a nucleation and growth rate controlled process in the electroformation of the Ag_2O layers. The present results allow to understand previous observations and throw further light on certain discrepancies about this matter still existant in the literature.

Acknowledgements—This work was financially supported by the Consejo Nacional de Investigaciones Científicas y Técnicas and the Comisión de Investigaciones Científicas de la Provincia de Buenos Aires.

REFERENCES

1. M. Lopez Teijelo, J. R. Vilche and A. J. Arvia, *J. electroanal. Chem.* **131**, 331 (1982).
2. B. V. Tilak, R. S. Perkins, H. A. Kozlowska and B. E. Conway, *Electrochim. Acta* **17**, 1447 (1972).
3. G. T. Bunstein and R. C. Newman, *Electrochim. Acta* **25**, 1009 (1980).
4. P. Stonehart, *Electrochim. Acta* **13**, 1879 (1968).
5. J. Zerbino, M. Lopez Teijelo, J. R. Vilche and A. J. Arvia, *Electrochim. Acta.* **30**, 1521 (1985).
6. J. M. M. Drogg, *J. electroanal. Chem.* **115**, 225 (1980).
7. G. W. D. Briggs, M. Fleischmann, D. J. Lax and H. R. Thirsk, *Trans. Faraday Soc.* **64**, 3128 (1968).
8. J. M. M. Drogg and F. Huisman, *J. electroanal. Chem.* **115**, 211 (1980).
9. R. H. Muller and C. G. Smith, *Surf. Sci.*, **96**, 375 (1980).
10. G. W. D. Briggs, M. Fleischmann, D. J. Lax and H. R. Thirsk, *Trans. Faraday Soc.* **64**, 3120 (1968).
11. J. C. Hamilton, J. C. Farmer and R. J. Anderson, *J. electrochem. Soc.* **133**, 739 (1986).
12. J. M. M. Drogg, P. T. Arderliesten and G. A. Bootsma, *J. electroanal. Chem.* **99**, 173 (1979).
13. B. G. Pound, D. D. McDonald and J. W. Tomlinson, *Electrochim. Acta* **25**, 1293 (1979).
14. R. S. Perkins, B. V. Tilak, B. E. Conway and H. A. Kozlowska, *Electrochim. Acta* **17**, 1471 (1972).
15. B. G. Pound, D. D. MacDonald and J. W. Tomlinson, *Electrochim. Acta* **25**, 563 (1980).
16. S. Fletcher and C. S. Halliday, *J. electroanal. Chem.* **159**, 267 (1983).
17. B. Scharifker and G. Hill, *Electrochim. Acta* **28**, 879 (1983).
18. B. Scharifker, R. Regules and J. Mozota, *Electrochim. Acta* **29**, 261 (1984).
19. B. G. Pound, D. D. MacDonald and J. W. Tomlinson, *Electrochim. Acta* **27**, 1489 (1982).
20. N. D. Rozenblyum, N. C. Bubyreva, V. I. Bukhareva and G. Z. Kazakevic, *Zh. Fiz. Khim.* **40**, 2467 (1966).